942211

A Three-Dimensional Head-Neck Model: Validation for Frontal and Lateral Impacts

M. de Jager and A. Sauren
Eindhoven University of Technology

J. Thunnissen
TNO Crash Safety Research Centre

J. Wismans
TNO Crash Safety Research Centre and Eindhoven University of Technology

ABSTRACT

The three-dimensional head-neck model of Deng and Goldsmith (J. Biomech., 1987) was adapted and implemented in the integrated multibody/finite element code MADYMO. The model comprises rigid head and vertebrae, connected by linear viscoelastic intervertebral joints and nonlinear elastic muscle elements. It was elaborately validated by comparing model responses with the responses of human volunteers subjected to frontal and lateral sled acceleration impacts. Fair agreement was found for both impacts. Further, a sensitivity analysis was performed to assess the effect of parameter variations on model response. The model proved satisfactory and may be used as a tool to improve restraint systems or dummy necks.

INTRODUCTION

Neck injuries frequently occur in automotive accidents, although the reported incidences may differ widely from one study to another. This may be due to regional differences, the considered time period, and database selection, among other factors. At one extreme, Ono and Kanno [1] reported that as much as half of the car-to-car impacts result in neck injuries, whereas, at the other extreme, Otte and Rether [2] found that only 2 % of the injured car occupants sustained neck injuries. Faverjon *et al.* [3] found neck injuries for 10 % of *all* front seat car occupants involved in an accident, and Bunketorp *et al.* [4] reported that 25% of the *injured* car occupants had neck injuries. In these studies, the majority of the neck injuries were rated as minor injuries (AIS = 1). Thus, severe neck injuries are uncommon in car accidents. However, one third of all injuries with permanent disability are neck injuries according to Lövsund *et al.* [5].

Neck injury is the most common injury in rear-end impacts [1,5]. These impacts make up half of the car-to-car impacts [6]. Approximately 10 % of all occupants involved in rear-end impacts sustain (minor) neck injuries [5]. These injuries are often referred to as whiplash injuries and they result in irritating complaints like forgetfulness, dizziness, and a stiff neck.

The mechanisms causing injuries to the neck are not fully understood as the neck is an anatomically and mechanically complex structure subjected to a variety of loading conditions in an accident. Both experimental research and mathematical modelling may aid in the understanding of neck injury mechanisms, see for example Refs. [7–9] and the reviews [10,11], respectively.

The major pitfalls in mathematical modelling of biological systems are oversophistication, lack of good physical properties data, and lack of validation [12]. Oversophistication will result in a model including too many details of which the effect on model behaviour may be difficult to retrieve. Physical properties should be based on experimentally obtained data to model the mechanical behaviour of the system realistically. Thus, due to the need to reduce model complexity and the lack of reliable physical properties data, numerous assumptions (and simplifications) have to be introduced into the model. To check on the assumptions, validation is needed. It is achieved by correlating numerical predictions with experimental results covering the situations for which the model will be used.

Three types of mathematical models have been used to describe the human head-neck response to impacts: two-pivot, discrete parameter, and finite element models.

Two-pivot models are relatively simple three-segment two-joint models of the head-neck-torso in which the neck is modelled as a rigid or an extensible link connecting head and torso. These models have been developed by Bosio and Bowman [13] and Wismans *et al.* [14,15] to analyze the response of human volunteers and cadavers in sled acceleration impacts. Pivot models are intended to describe the global motion of head and neck relative to the torso. To describe vertebral kinematics and soft tissue deformations, more detailed models are needed.

In discrete parameter models, head and vertebrae are represented by rigid bodies that are connected by mass-

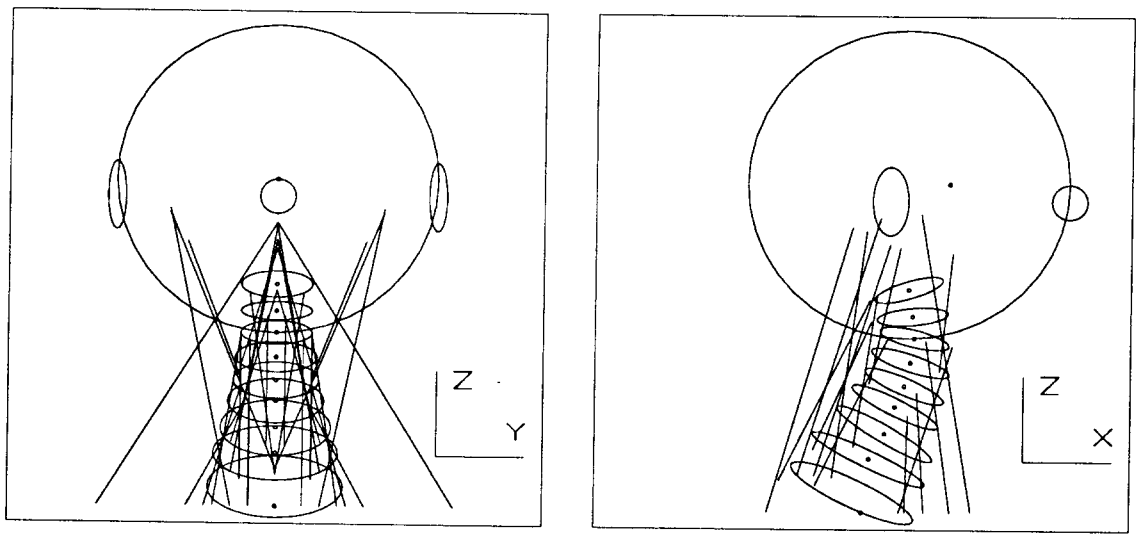

Figure 1: Frontal and lateral view of model. Ellipsoids represent the vertebrae, the large circle the skull (including nose and ears for visual purposes). The small circles show the centres of gravity for each body. Lines denote the muscle elements.

less deformable elements representing the intervertebral soft tissues and muscles. These models have been developed by Tien and Huston [16] and Deng and Goldsmith [17] among others.

In finite element models of the neck, as developed by Williams and Belytschko [18] and recently by Kleinberger [19], a highly detailed representation of cervical spine geometry and material behaviour may be employed. These models are complex and have many parameters, which makes them computationally less efficient and more difficult to validate than discrete parameter models.

A discrete parameter model is complex enough to include vertebral deformations, but simple enough to be comprehensible, that is to understand how certain modelling choices and model parameters affect the model behaviour. As more insight is gained, model complexity may be increased by including more details to obtain a more realistic model.

This two-phase approach is used at the Eindhoven University of Technology to develop a three-dimensional head-neck model describing the mechanical behaviour of the human head-neck system in impact situations such as occur in car crashes. In the first phase, a relatively simple discrete parameter model describing the global head motion is developed. This global model may be used for example as a tool to improve restraint systems or dummy necks. In the second phase, the model will be refined by including detailed representations of the mechanically relevant soft tissues. This detailed model may be used to gain insight into vertebral kinematics, soft tissue loads, and injury mechanisms.

In this paper, the global model is dealt with. It was chosen to start with the model of Deng and Goldsmith as it looked promising. The model was modified and implemented in MADYMO. Validation was carried out by comparing model responses with human volunteer responses to frontal and lateral acceleration impacts. Subsequently, a sensitivity analysis was performed.

First, a short description of the model and the introduced modifications are given. Second, human volunteer response envelopes are described. These envelopes specify the response patterns for frontal and lateral impacts the model has to meet to be valid. After presentation of some simulation results, the model and the results are discussed. Finally, a summary and conclusions are given.

HEAD-NECK MODEL

The three-dimensional discrete parameter model of Deng and Goldsmith [17] is a mid-sagittal symmetrical model describing the dynamic behaviour of the human head and neck subjected to acceleration impacts. It comprises ten rigid bodies, representing head, cervical vertebrae C1 through C7, thoracic vertebra T1, and thoracic vertebra T2 including the thorax. The bodies are connected by linear viscoelastic elements representing the intervertebral joints. The major neck muscles are included by 15 symmetrical pairs of nonlinear elastic elements.

The model was modified mainly to remove some inaccuracies, and implemented in the integrated multibody/finite element code MADYMO, version 5.1, of the TNO Crash-Safety Research Centre [20]. A frontal and lateral view of the model is depicted in Fig. 1. Model and modifications are described in brief in the following sections. For more details, the reader is referred to the original publications [17,21]. For the sake of clarity and completeness, all data needed to reproduce the model are reproduced in this paper. The data not given in Deng and Goldsmith [17] could be extracted from Deng [21].

Table 1: Rigid body data.

Body Nr.	Name	Mass (kg)	I_{xx}	I_{yy}	I_{zz} ($10^{-4}kgm^2$)	s_x	s_y	s_z ($10^{-2}m$)	g_x	g_y	g_z ($10^{-2}m$)	θ_y (deg)
1	Thorax (T2)	—	—	—	—	—	—	—	0.	0.	0.00	0.00
2	T1	1.000	49.0	14.0	61.0	0.00	0.	2.28	0.	0.	0.92	25.75
3	C7	0.400	21.0	6.0	26.0	0.07	0.	1.78	0.	0.	0.86	5.00
4	C6	0.226	5.0	5.3	9.7	-0.26	0.	1.72	0.	0.	0.79	-3.50
5	C5	0.269	6.0	4.8	10.0	-0.07	0.	1.45	0.	0.	0.66	-3.25
6	C4	0.205	2.5	3.7	5.7	-0.20	0.	1.39	0.	0.	0.66	-5.00
7	C3	0.156	3.3	2.6	4.3	-0.20	0.	1.35	0.	0.	0.73	-5.00
8	C2	0.156	3.3	2.6	4.3	-0.20	0.	1.32	0.	0.	0.66	-19.50
9	C1	0.156	3.3	2.6	4.3	0.07	0.	1.58	0.	0.	0.66	-12.00
10	Head (C0)	3.500	353.0	516.0	516.0	0.13	0.	1.32	0.	0.	6.34	17.50

RIGID HEAD AND VERTEBRAE Rigid bodies are used to represent the head and vertebrae. The sequence of numbering of the ten rigid bodies is given in Table 1. Body 1, in the lowest position, represents vertebra T2 and the torso, and serves as the base (or origin) of the system.

The initial configuration of the bodies includes the cervical lordotic curvature and was based on X-ray radiographs. The relative position and orientation of each body are described relative to its adjacent lower numbered body. Therefore, a local coordinate system is assigned to each body. The local coordinate system of body T2 is called the reference coordinate system; the x, y, z-axes of it point in forward, left, and upward directions respectively. The origin of the local coordinate system of body j is defined relative to the coordinate system origin of the lower numbered body i by the coordinates s_x, s_y, s_z expressed in the lower body coordinate system, see Fig. 2 and Table 1. The relative orientation is given by the angle θ_y about the y-axis of the lower body. The coordinate system origins are positioned in between two vertebrae, close to the facet joints and posterior edge of the intervertebral disc.

The inertial properties of the system are lumped into the rigid bodies. The mass (m) and moments of inertia (I) of the bodies were based on a study by Liu *et al.* [22]. The position of the centre of gravity (cg) of body j is given relative to the local coordinate system of body j by the coordinates g_x, g_y, g_z, see Fig. 2 and Table 1. The principal moments of inertia are defined with respect to a coordinate system with its origin at the cg and parallel to the body local coordinate system (Table 1). Thus, the orientation of the body coordinate system axes were chosen such that they resemble the principal inertia axes. The inertia moments given by Deng for bodies C4, C5 and C6 were slightly modified to fulfil the requirements for rigid body inertia moments, i.e. $I_{ii} + I_{jj} \geq I_{kk}$ for $i, j, k = x, y, z$ and $i \neq j \neq k$ [23].

LINEAR VISCOELASTIC INTERVERTEBRAL JOINT MODEL The rigid bodies are connected by a linear viscoelastic model representing the mechanical behaviour of the intervertebral soft tissues, thus expressing motion segment behaviour.

The compound behaviour of intervertebral disc, ligaments, and facet joints is modelled by a stiffness and a damping matrix relating the three-dimensional deformations of a joint to loads applied to the upper and lower vertebra of that joint. The relationship between loads and deformations is given by

$$\begin{bmatrix} f_x \\ f_y \\ f_z \\ m_x \\ m_y \\ m_z \end{bmatrix} = A \cdot \left(\begin{bmatrix} k_{11} & 0 & k_{13} & 0 & k_{15} & 0 \\ & k_{22} & 0 & k_{24} & 0 & k_{26} \\ & & k_{33} & 0 & k_{35} & 0 \\ & & & k_{44} & 0 & k_{46} \\ & symmetrical & & & k_{55} & 0 \\ & & & & & k_{66} \end{bmatrix} \begin{bmatrix} t_x \\ t_y \\ t_z \\ \phi_x \\ \phi_y \\ \phi_z \end{bmatrix} + \begin{bmatrix} d_{11} & 0 & 0 & 0 & 0 & 0 \\ & d_{22} & 0 & 0 & 0 & 0 \\ & & d_{33} & 0 & 0 & 0 \\ & & & d_{44} & 0 & 0 \\ & symmetrical & & & d_{55} & 0 \\ & & & & & d_{66} \end{bmatrix} \begin{bmatrix} v_x \\ v_y \\ v_z \\ \omega_x \\ \omega_y \\ \omega_z \end{bmatrix} \right),$$

in which f_i and m_i ($i = x, y, z$) are the components of the forces and moments with respect to the i-axis of the lower body, while t_i and ϕ_i are the relative translational and rotational displacements and v_i and ω_i the relative translational and rotational velocities of the upper body relative to the lower body. Factor A is used to account for variation in mechanical properties of the joint with vertebral level.

Joint Displacement – The relative translations and rotations have to be determined to calculate the joint loads. The translation of the upper body is defined as the translation of its coordinate system origin relative to the lower body coordinate system. It is measured relative to the point given by the coordinates g_x, g_y, g_z in the lower body coordinate system. This point is fixed to the lower body and resembles the initial position of the upper body coordinate system origin. The calculated loads are applied to both bodies at this point.

Deng used Bryant angles to resolve the relative three-dimensional orientation of the bodies into three rotation components. With this method, all three components are described relative to differently orientated coordinate

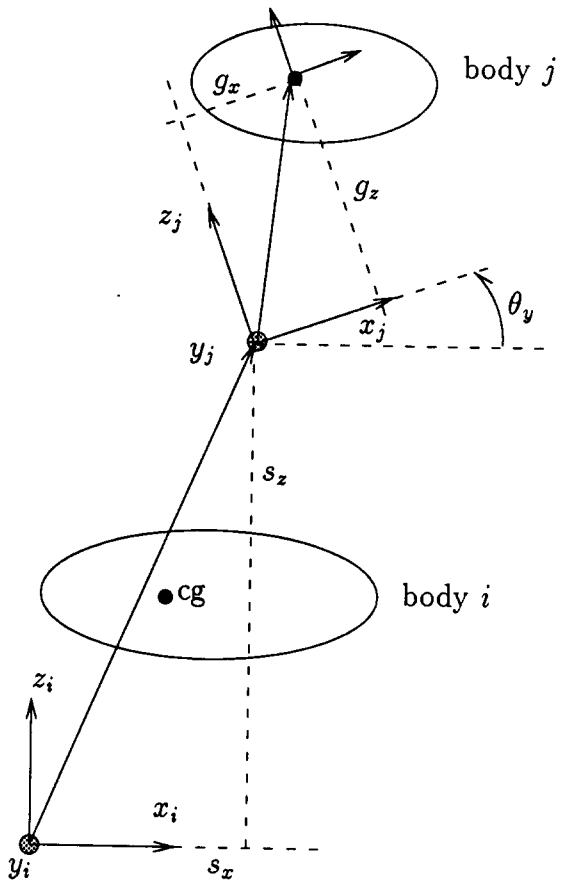

Figure 2: Definition of body local coordinate systems and centre of gravity positions.

systems. The first component is a rotation about the i-axis of the lower body coordinate system, the second rotation is about the j-axis of an intermediate coordinate system, and the third rotation is about the k-axis of the upper body coordinate system (with $i \neq j \neq k$).

Although any of the six combinations for which $i \neq j \neq k$ may be chosen, the occurrence of singularities should be avoided. This gimbal lock occurs when the rotation about the j-axis equals $\pi/2$. Then the i- and k-axis are parallel and the rotation angles about these axes cannot be uniquely determined.

For intervertebral deformations, it is unlikely that any of the rotations will approximate $\pi/2$. However, the method is also used to resolve the head rotation relative to the torso. The forward rotation (about the y-axis) and sideward rotation (about the x-axis) of the head may exceed $\pi/2$ in frontal and lateral impacts, respectively. The axial head rotation (about the z-axis), on the contrary, is thought to remain well below $\pi/2$, for these impacts — and other impacts as well. Therefore, the order $i = y, j = z, k = x$ was chosen, which agrees with the order used by Deng.

Joint Stiffness – For linear elastic material behaviour, the stiffness matrix K should be symmetrical. The off-diagonal elements account for coupling of deformations in one direction with loads in another. They allow the coupling phenomenon observed in the cervical spine to be incorporated into the model. The zero-elements follow from sagittal plane symmetry.

Originally, Deng used bi-linear stiffness coefficients to account for different stiffnesses for deformations along or about the same axis but with opposite of sign, e.g. flexion and extension. Following Panjabi *et al.* [24], Deng used two symmetrical stiffness matrices: one (K^+) with stiffness coefficients valid for positive relative deformations ($t_i, \phi_i > 0$), and one (K^-) with coefficients valid for negative relative deformations ($t_i, \phi_i < 0$). However, in simulations, both positive and negative deformations may occur at the same time, in which case the momentaneous stiffness matrix K has to be assembled columnwise from K^+ and K^-. For the positive deformations, the corresponding columns are taken from K^+, and for the negative directions from K^-, resulting in a stiffness matrix K in which the coupling coefficients are non-symmetrical. For example, assume ϕ_y to be positive and t_x to be negative, then coefficient k_{15} (relating ϕ_y to f_x) is taken from K^+ and may be different from k_{51} (relating t_x to m_y) taken from K^-.

Here, this problem is solved using one stiffness matrix of which only the diagonal elements are bi-linear. Taking mid-sagittal plane symmetry into account, this makes sense only for non-symmetrical deformations. The stiffness matrix is then given by

$$K = \left[\begin{array}{ccc|ccc} k_{11} & 0 & 8\cdot10^3 & 0 & -800 & 0 \\ & 122\cdot10^3 & 0 & 450 & 0 & 300 \\ & & k_{33} & 0 & -380 & 0 \\ \hline & & & 171.9 & 0 & -1.5 \\ & \textit{symmetrical} & & & k_{55} & 0 \\ & & & & & 149 \end{array}\right]$$

$$\left[\begin{array}{c|c} N/m & N/rad \\ \hline N & Nm/rad \end{array}\right],$$

with

$$k_{11} = \begin{cases} 140\cdot10^3\ N/m & \text{for } t_x \geq 0 \text{ posterior/ant. shear} \\ 50\cdot10^3\ N/m & \text{for } t_x < 0 \text{ anterior/post. shear} \end{cases}$$

$$k_{33} = \begin{cases} 390\cdot10^3\ N/m & \text{for } t_z \geq 0 \text{ tension} \\ 1083\cdot10^3\ N/m & \text{for } t_z < 0 \text{ compression} \end{cases}$$

$$k_{55} = \begin{cases} 151.8\ Nm/rad & \text{for } \phi_y \geq 0 \text{ flexion} \\ 185.6\ Nm/rad & \text{for } \phi_y < 0 \text{ extension} \end{cases}$$

All values were taken from Deng, who has derived them primarily from the results of experiments on thoracic motion segments reported by Panjabi *et al.* [24]. The values for the off-diagonal elements are the average values of the 'positive' and 'negative' coefficients given by Deng. The damping coefficients have the values $d_{11} = d_{22} = d_{33} = 300\ Ns/m$ and $d_{44} = d_{55} = d_{66} = 1.0\ Nms/rad$.

The same model is applied to all joints. However, the matrices are multiplied by a proportionality factor A

Table 3: Muscle elements data.

Muscle	O	x	y	z	I	x	y	z	A
			(cm)				(cm)		(cm^2)
sternocleidomastoideus	1	6.14	2.5	0.00	10	0.73	6.0	3.77	3.586
longus capitis	6	1.72	2.0	0.66	10	2.51	0.0	1.45	2.000
longus colli	1	2.11	1.5	0.00	7	2.18	1.5	0.79	2.000
scalenus anterior	7	0.66	2.0	0.73	1	4.96	3.5	0.00	1.656
scalenus medius	5	0.79	2.0	0.59	1	3.50	4.0	0.00	0.436
scalenus posterior	4	0.86	2.0	0.66	1	2.44	5.0	0.00	1.360
trapezius	1	-5.29	10.0	0.00	10	-3.10	0.0	2.97	3.500
splenius capitis	1	-3.57	0.0	2.18	10	-1.52	6.0	3.57	2.244
splenius cervicis	1	-4.62	0.0	1.85	9	-2.25	1.5	0.73	0.847
spinalis capitis	1	-2.64	2.5	2.11	10	-0.99	0.0	1.98	0.800
spinalis cervicis	2	-3.04	0.5	0.00	8	-2.31	0.5	0.59	0.800
semispinalis capitis	1	-1.65	2.5	1.98	10	-2.31	0.0	2.78	1.500
semispinalis cervicis	2	-1.06	2.5	1.12	9	-1.78	0.0	0.86	0.718
longissimus capitis	5	-1.85	2.0	0.00	10	-0.40	5.0	1.85	0.800
longissimus cervicis	1	-2.58	2.0	1.59	7	-1.45	2.0	0.33	0.800

O: origin I: insertion A: average cross-sectional area

Table 2: Joint factor A.

Joint	A (-)	Joint	A (-)	Joint	A (-)
C0-C1	3.11	C3-C4	1.38	C6-C7	1.84
C1-C2	2.31	C4-C5	1.27	C7-T1	1.98
C2-C3	1.00	C5-C6	1.51	T1-T2	0.50

to account for the variability in mechanical properties with vertebral level, which Panjabi *et al.* [24] found for thoracic segments. Deng based this factor on the cross-sectional area of the intervertebral discs, with C2-C3 as reference value (Table 2). Factor T2-T1 takes the thorax flexibility into account. Note the relatively high factors for the atlanto-axial (C1-C2) and atlanto-occipital (C1-C0) joints.

NONLINEAR ELASTIC MUSCLE ELEMENTS The major neck muscles are incorporated into the model by fifteen symmetrical pairs of nonlinear elastic elements. Only passive muscle behaviour is modelled, so (neural activation of) muscle contraction cannot be simulated.

The muscles are modelled as springs with a nonlinear force-deformation relationship. The coordinates of origin and insertion are expressed relative to the local coordinate system of the body to which they are attached, see Table 3. Originally, Deng modelled the muscles as three-point elements: besides the endpoints, a third intermediate point was used to allow for more realistic force directions as to simulate the curvature of the muscles around bones. However, Deng did not allow muscle forces to act on this midpoint. This can not be reproduced in MADYMO using standard elements. Either the midpoint is omitted, or it is included with muscle forces acting on it. Although a muscle will exert forces on the vertebrae around which it curves, it is felt inappropriate to have this force act only on the vertebra to which the midpoint is connected. For sufficiently large forces, this may cause the vertebra to be squeezed out of surrounding vertebrae. Therefore, the midpoint was not included in the present model.

Passive muscle behaviour is modelled by the nonlinear stress-strain relationship

$$s = \begin{cases} \dfrac{ke}{1 - e/a} & \text{for } e > 0 \\ 0 & \text{for } e \leq 0 \end{cases},$$

with s the muscle stress due to strain e (i.e. elongation relative to reference length), k the muscle stiffness constant, and a the strain asymptote. By setting $k = 3.34 \cdot 10^4\ N/m^2$ and $a = 0.7$, Deng was able to reproduce the experimentally found stress-strain curve for the sternocleidomastoid presented by Yamada [25]. All muscles have the same stress-strain characteristic. The muscle force is obtained through multiplication of the muscle stress by the muscle cross-sectional area A. The values are listed in Table 3 and were obtained from various sources. Finally, to account for the muscle activity needed to keep head and neck in an upright position, stiffness k was multiplied by a factor 10.

HUMAN VOLUNTEER RESPONSE ENVELOPES

The model has to be validated to check its capability to predict the dynamic response of the human head and neck to impacts. Validation is achieved by correlating model responses with experimentally obtained head-neck responses.

Deng validated his model using one single volunteer response to a frontal sled acceleration test and one response to a lateral sled test. The response patterns were in reasonable agreement. However, the head accelerations remained well below those from the volunteer during the first phase of the impact. In the present study,

response envelopes based on numerous human volunteer sled acceleration tests are used. These envelopes specify the response patterns the model has to meet to be valid.

The envelopes are based upon the head-neck responses obtained from human volunteer sled acceleration tests performed at the Naval Biodynamics Laboratory (NBDL), e.g. Ewing and Thomas [26]. At the NBDL, an extensive series of impact tests has been performed with male human volunteers to obtain head-neck responses for various levels and directions of impact. In these tests, the volunteer was seated on a sled. Straps were used to prevent torso motion adequately. Head and neck were allowed to move freely in response to the impact applied by accelerating the sled from zero velocity. The three-dimensional accelerations and displacements of head and vertebra T1 were monitored using accelerometers and high speed film.

Impacts have been conducted for frontal, lateral, and oblique directions. An analysis of a subset of these tests was performed by Wismans *et al.* [14] using a two-pivot model of the head-neck system. They analyzed the more severe impacts in frontal, lateral, and oblique directions. In the present study, the same subsets for frontal and lateral impacts are used. For frontal impacts, the results of tests in which the peak sled acceleration was 14 g ($g = 9.81\,m/s^2$) or higher are used; these are nine tests with five volunteers. For lateral impacts, the results of tests with peak sled acceleration of 7 g or higher are used; these are nine tests with nine volunteers. It was observed that the measured T1-acceleration differed from the applied sled acceleration, due to the flexibility of straps and thorax. The peak T1-accelerations were twice as high as the peak sled accelerations. More details about the tests and results may be found in Wismans *et al.* [14] and Wismans and Beusenberg [27].

To validate the model, a sled test is simulated and the model response is compared to the volunteer response envelopes. To simulate the test, the average measured horizontal T1-acceleration (in impact direction) is used as input to the model. This circumvents the need to model the straps and thorax flexibility. The vertical T1-accelerations are small enough to be neglected. For the frontal impacts, considerable rotation of T1 in the impact direction was observed. Here, this rotation was not taken into account.

The response envelopes are defined as follows. For all tests, the obtained volunteer responses were pooled. The envelopes were then determined as the upper and lower boundaries of the pooled responses. Thus, the envelopes are the corridors in between which each volunteer response is found. To have a sufficiently accurate model, the model response should be close to the envelopes.

The following response envelopes are considered:

- The linear and angular accelerations of the head centre of gravity (cg) relative to the laboratory coordinate system (resultant acceleration and its x, y, z-components). The x, y, z-axes of this non-moving coordinate system point to the forward, left, and upward direction. Note that in the acceleration envelopes, the sled acceleration is included as well.
- The linear and angular displacements of the head cg relative to the T1-anatomical coordinate system (resultant displacement and its x, y, z-components). This coordinate system is positioned at the middle of the anterior edge of the T1 vertebral body. It is, and remains, orientated parallel to the laboratory coordinate system.
- The head-rotation history and, for the frontal impact only, the neck- versus head-rotation (head lag). Head rotation is measured relative to the torso, i.e. to the T1-anatomical coordinate system. Neck rotation is defined as the rotation of the neck link of the two-pivot model used to analyze the responses. The link connects the occipital condyles (oc) to the centre of the circular arc approximating the oc-trajectory. This centre of rotation was found to be close to the T1-anatomical coordinate system. See Wismans *et al.* [14] for more details.

ADDITIONAL MODEL MODIFICATIONS Some model modifications have to be introduced to validate the model properly using the envelopes described above.

The inertial properties of the head and the position of the head cg were changed to match the average volunteer properties given by Wismans *et al.* [14]. As before, the inertia moments are expressed relative to a coordinate system positioned at the cg with the same orientation as the body local coordinate system. To this end, the data given by Wismans *et al.* were converted to match this situation. In Table 4, both the converted data and the data used by Deng are given. Obviously, the volunteer head mass is larger while the moments of inertia are smaller than those used by Deng.

Because the average T1-acceleration history is used to simulate the impacts, the T1-body has to be the system's reference body. This is realized by rigidly attaching body T1 to T2 in the model. Further, in the model, the T1-anatomical coordinate system was introduced, which was given the same position as the T1 body local coordinate system but the same orientation as the laboratory and T2-reference coordinate systems. Neck rotation is then defined as rotation of the line connecting the C0-C1 joint to the origin of the T1-anatomical coordinate system.

Gravity ($g = 9.81\ m/s^2$) was included.

Table 4: Head inertial data.

author	mass	I_{xx}	I_{yy}	I_{zz}	I_{yz}	g_x	g_z
	(kg)	$(10^{-4} kgm^2)$				(cm)	
Deng	3.500	353	516	516	–	0.00	6.34
Wismans[1]	4.780	186	246	183	73	2.30	5.50

[1] with correction for instrumentation (with mass of 0.53 kg)

RESULTS

Several simulations were performed with the model using MADYMO version 5.1 on a Silicon Graphics Personal Iris 4D30 Workstation. For simulations as those described below, CPU-times are typically less than ten minutes.

To start with, the frontal and lateral impacts reported by Deng were simulated. Model responses are compared to those reported by Deng to see how the modified model corresponds with Deng's model.

The third and fourth simulation reproduce the frontal and lateral sled impacts. Model responses are compared to the response envelopes to validate the model. For these two simulations only, the additional modifications described above were introduced.

Numerous other simulations were performed in which one or more model parameters were changed to assess the sensitivity of model response to parameter variations. Results of this sensitivity analysis are summarized below.

DENG FRONTAL AND LATERAL IMPACT The results for the frontal and lateral impact used by Deng are depicted in Fig. 5 and 6, respectively. A dashed line was used for Deng's results and a solid line for the responses of the present model.

For the frontal impact, Fig. 5a shows the sled acceleration history applied to the model at T2. Fig. 5b,c,d respectively show the x- and z-component of the linear acceleration and the angular acceleration of the head cg relative to a non-moving coordinate system parallel to the T2 coordinate system. The corresponding displacements and rotations relative to T2 are given in Fig. 5f,g,h, while Fig. 5e shows the head trajectory within the sagittal plane.

For the lateral impact, the applied sled acceleration is given in Fig. 6a. The x-, y-, and z-components of the resulting head cg accelerations and displacements, are presented in Fig. 6b,c,d and f,g,h, respectively. It should be noted that the head cg y-acceleration reported by Deng did not include the sled acceleration. Here, this was corrected for simply by adding the sled acceleration to Deng's results. Fig. 6e shows the trajectory projected onto the frontal plane.

For both impacts, the following is observed. During the first 120 ms, the model closely follows the results of Deng, but then a deviation between the responses occurs. Qualitatively, the response patterns are similar, only a shift in time occurs. Quantitatively, the peak values are somewhat larger for the present model: the model is more flexible than Deng's model. This is clearly revealed by the head cg trajectory.

In search for the causes of the found differences, several model adaptations were introduced temporarily to bring the simulation results more closely to those of Deng. The most important adaptation was the use of three-point muscle elements with forces acting on the midpoint, which is different from Deng's model. It was found that the difference in response could only partially be explained through the differing muscle representations. For a given deformation, the two-point representation results in lower strains than the three-point representation would have resulted in. Lower strains imply lower forces and, consequently, less resistance to deformation and a more flexible model. The two-point representation also gives different force directions, and this may influence the response as well.

In conclusion, the model of Deng and Goldsmith was reproduced with some modifications. Response patterns were found to be similar, but reflected a difference in flexibility partly due to the differing muscle representation.

VOLUNTEER FRONTAL IMPACT This simulation represents the average frontal impact conducted with human volunteers. Fig. 3 depicts the model configurations during the first phase (40-180 ms) of the impact in 20 ms intervals. In Fig. 7 the results are quantified. Fig. 7a shows the average T1-acceleration applied to the model to simulate the frontal impact. Fig. 7b–h show both the model responses (solid line) and the volunteer envelopes (dashed lines). Ideally, the model response should fall in between the envelopes.

Fig. 7b,c,d respectively show the x- and z-component and the resultant linear acceleration of the head cg relative to the laboratory coordinate system. Fig. 7e shows the head angular acceleration in the sagittal plane, i.e. about the y-axis. In general, the accelerations agree fairly well with the envelopes. For the x-component and the resultant linear acceleration, a qualitatively good correspondence between model response and volunteer envelopes is found up to 200 ms. However, correspondence is less good for the z-acceleration. The model response starts somewhat late and does not reflect the fluctuation of the volunteer envelopes around 110 ms, although the maximum and minimum peak accelerations correspond well with the envelopes. For the angular acceleration, correspondence in a qualitative sense is reasonable up to 150 ms. The acceleration increases too early, causing the maximum to occur somewhat too soon, although it falls in between the envelopes. The decrease then is fast enough, but levels out too soon. After 200 ms, when the impact is almost over, the model still shows oscillating behaviour, while the volunteers apparently tend to bring back their head and neck in an upright position by actively contracting their muscles. As this cannot be simulated with the model, its oscillation slowly damps out.

The trajectory (Fig. 7f) reveals that the model's head cg follows a less circular path than the volunteers head cg, which may be due to larger neck elongation in the model. Also, the average neck length differs between model and volunteers. The head rotation (Fig. 7g) increases too soon, which is also reflected by the head lag

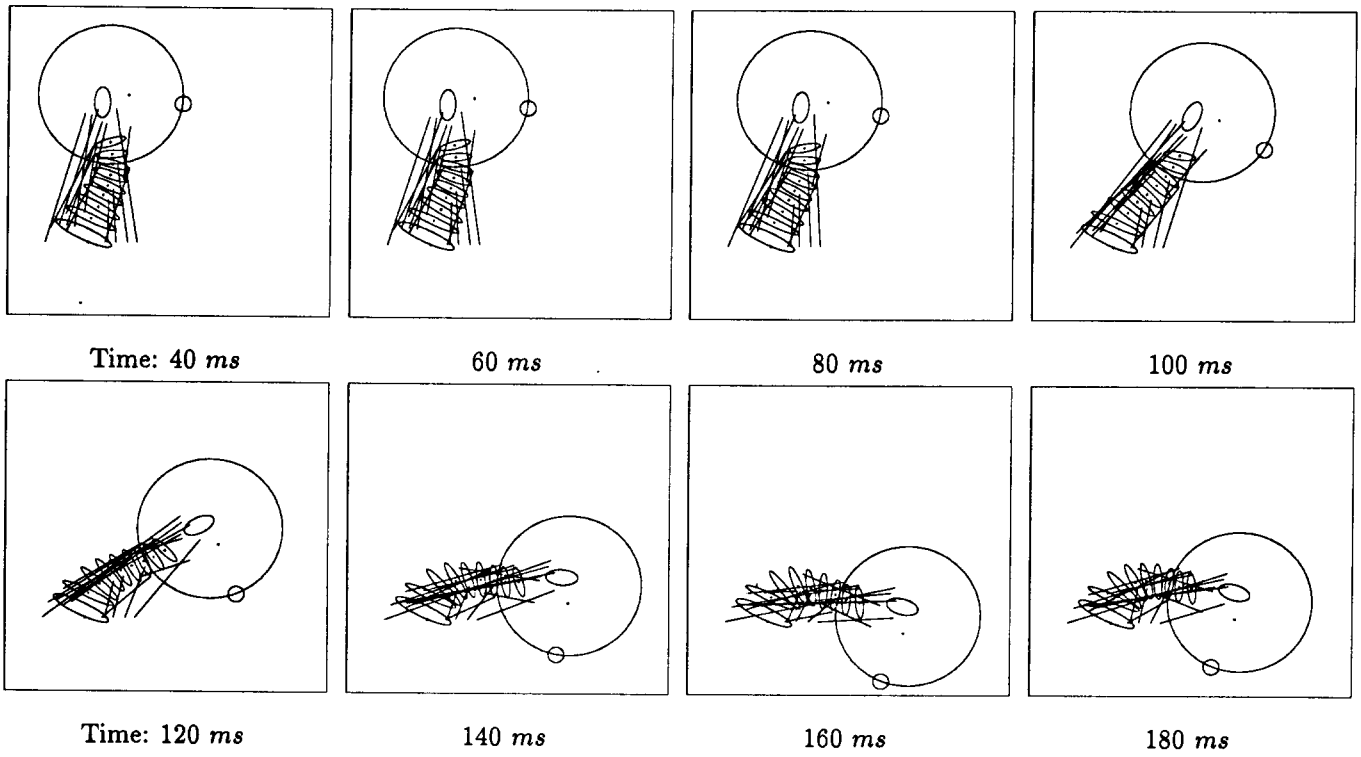

Figure 3: Model configurations for volunteer frontal impact.

(Fig. 7h). Head and neck rotation seem to be coupled in the model, whereas for the volunteers the head rotation lags considerably behind the neck rotation. First, the head translates only in the direction of impact due to inertial loading, then it is forced to follow the fully stretched neck (i.e. without lordosis) and hence to rotate. Thus, the head lag is not well represented by the model. The most likely cause of this omission is the strong coupling between head and neck due to the chosen joint model and proportionality factor for the C0-C1 joint. This does not only cause the head lag to be incorrect, but also the head angular acceleration to increase too soon and the z-acceleration to respond too late. It is felt that a more realistic modelling of the C0-C1 joint will improve the results at this point.

In brief, fair agreement between model and volunteer responses is found, except for the head lag that is not properly reflected by the model. This is probably due to inappropriate modelling of the atlanto-occipital joint.

VOLUNTEER LATERAL IMPACT This simulation represents the average lateral impact performed with volunteers. Fig. 8a shows the average T1-acceleration that was used to simulate the impact. Fig. 8b,c,d, and e,f,g respectively show the components of the linear and angular acceleration of the head cg relative to the laboratory coordinate system. Fig. 8h,i,j and k,l,m respectively show the translational and rotational displacements of the head cg relative to the T1-anatomical coordinate system.

In general, qualitative agreement is good for the linear accelerations and displacements, and reasonable for the angular accelerations. Correspondence for the head rotation is less good. For the linear accelerations, the forward (x) component almost entirely lies within the envelopes, although the timing of the response is somewhat shifted. The lateral (y) component increases relatively late. Moreover, it does not show a significant drop around 150 ms: instead of a two-peak response, a wide and flattened response peak is found. For the vertical (z) component, the first (negative) peak is too large, but the timing is good.

For the angular acceleration, the second peak (150 ms) of the x-component does not agree with the envelopes. The y- and z-component show the same pattern as the envelopes, but slightly shifted in time. The peak sizes correspond well with the envelopes.

For all displacement components, the response patterns resemble the envelopes. Obviously, the starting points differ, due to different neck lengths for model and volunteers. Apart from this, good agreement is obtained, although the lateral (y) displacement lags somewhat behind the volunteer response. For the rotations, significant differences are found. The lateral (x) rotation of the head is almost twice as large as found for the volunteers, whereas the axial (z) rotation is much smaller. The forward (y) rotation differs little from the volunteers response. It should be noted that the head rotations were determined using the same order as was used to determine the volunteer head rotations, i.e. $i = x, j = z, k = y$.

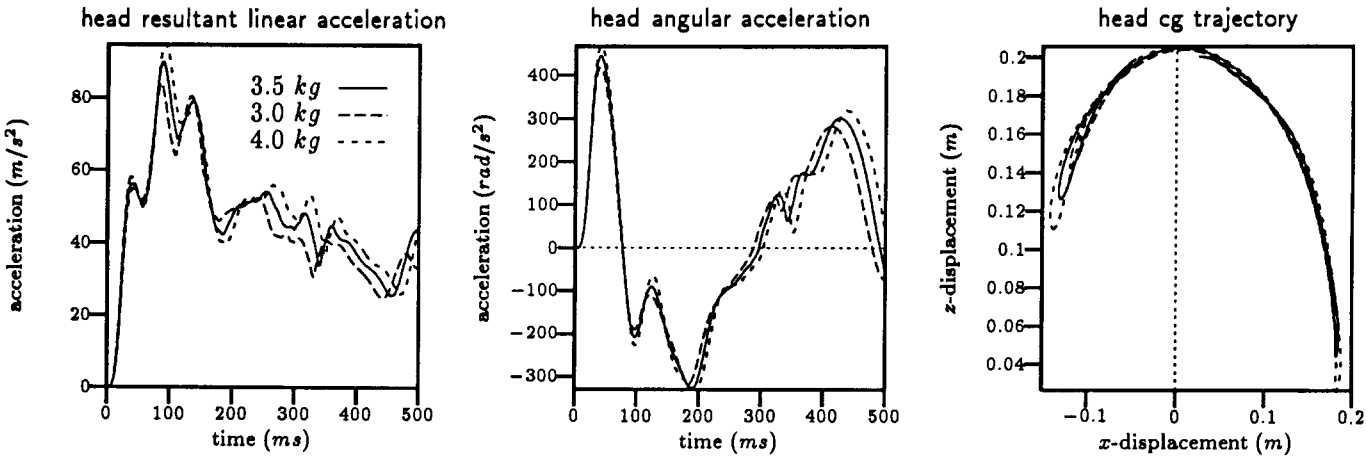

Figure 4: Results of head mass variation.

To summarize, reasonable agreement is obtained for the lateral impact as well. Lateral impacts are more difficult to describe than frontal impacts, due to the three-dimensional motion involved.

SENSITIVITY ANALYSIS A sensitivity analysis was performed to assess the sensitivity of model response to variations in one or more parameters. Parameters were varied one by one and the model response was compared to the response obtained for the first simulation (Deng frontal impact).

The following parameters were considered: head and vertebral masses, intervertebral joint stiffness and damping coefficients, joint proportionality factor, and muscle stiffness. Table 5 summarizes the performed variations: the first column gives the varied parameter; the second the amount of variation; the third the absolute influence on the model response — qualitatively in terms of large, moderate or small influence; and the fourth column the relative influence when compared to the influence of the head mass variation — again qualitatively in terms of similar, smaller, or negligible influence. Fig. 4 depicts the effect of head mass variation on the head cg trajectory, and the angular and resultant linear acceleration.

Table 5: Results of sensitivity analysis.

parameter	variation*	influence	relative influence
head mass	$\pm 0.5kg$	large	—
mass cervical vertebra			
- one	50, 200 %	small	negligible
- all together	50, 200 %	large	smaller
joint stiffness			
- k_{11}	80, 125 %	moderate	smaller
- k_{33}	80, 125 %	small	negligible
- k_{55}	80, 125 %	large	similar
- coupling coefficients	omitted	moderate	smaller
joint damping			
- d_{11}	50, 200 %	large	smaller
- d_{33}	50, 200 %	moderate	negligible
- d_{55}	50, 200 %	large	similar
joint factor			
- all joints	90, 110 %	large	smaller
- T2-T1 joint	80, 120 %	large	smaller
muscle stiffness	50, 200 %	moderate	smaller

* percentages as percentage of original value

Variation of the head mass has a considerable influence on the model response, which is to be expected as it is the major inertial force putting load into the system in impact situations. Variations of vertebral masses have little influence on the model responses, which confirms the findings of Deng. Variations of the joint stiffness and damping coefficients with respect to rotational deformations have a relatively large influence: most of the deformation of the model stems from relative rotation between the vertebrae. The anterior-posterior shear coefficient variations have a moderate influence, and the compression/tension coefficient variations have a negligible influence. The joint proportionality factor scales all stiffness and damping coefficients of the joint model together. Variations of the factor have a considerable influence although less than the head mass variation. The muscle stiffness variation shows a moderate influence of muscle forces on model response.

Additionally, the effect of the coupling coefficients on the model response for both the Deng frontal and lateral impact was studied. This was done by omitting all these coefficients which resulted in a diagonal stiffness matrix. The influence on the model response for both impacts was found to be moderate and somewhat smaller than the influence of the head mass variation on the response.

DISCUSSION

The three-dimensional discrete parameter model of Deng and Goldsmith was modified and reproduced. The model includes head and vertebrae as rigid bodies, the inter-

vertebral joints as three-dimensional linear viscoelastic elements, and the major neck muscles as nonlinear elastic elements. The model was validated for frontal and lateral impacts.

JOINT MODEL The joints are modelled by a stiffness and damping matrix relating the three-dimensional translational and rotational deformations of a joint to forces and moments applied to the upper and lower vertebra of the joint. Each joint was given the same stiffness ratios. This seems a valid approach for the lower cervical joints, C2-C3 through C7-T1, as they have the same structural characteristics. For the atlanto-axial (C1-C2) and atlanto-occipital (C1-C0) joints, however, this approach does not take the different and unique structural properties of these joints into account. To apply the same joint model, unique stiffness matrices should be used to account for the relatively large flexibility (and range of motion) for flexion-extension in the C1-C0 joint and for axial rotation in the C1-C2 joint. The coefficients may partly be based on recently reported experimental data characterizing the mechanical behaviour of these joints [28–30]. It is felt that this will improve the model response for frontal impacts regarding the head lag.

In the joint model, a proportionality factor was introduced to account for (assumed) variation of stiffness with vertebral level. This variation was found for thoracic motion segments [24], the results of which were used by Deng since little cervical data on motion segment behaviour was available. To date, more data on the (quasi)static characteristics of cervical motion segments are available which may be used to determine both stiffness coefficients and proportionality factors [31–33]. Remarkably, for quasistatic loads, a significant variation of segment stiffness with vertebral level was found in some directions [33], while for static loads, no significant variation was found [31, 32].

The major drawback of the used joint model is its linearity. The results reported by Shea *et al.* [33] show that the mechanical behaviour of motion segments is nonlinear under quasistatic loading. Similar to what has been found for spinal ligaments [34] and the occipito-atlanto-axial complex [29], the force-displacement characteristics typically have a sigmoidal shape, expressing an initial low resistance to deformation (neutral zone) followed by an increasing resistance until the end of the range of motion. Deformations beyond this range of motion will usually result in structural failure (injury) of the segment. To take this nonlinear behaviour into account, the diagonal stiffness coefficients in the joint model may be varied with varying deformation to represent the sigmoidal force-displacement curve more closely than constant coefficients do.

MUSCLE ELEMENTS The muscles are modelled as nonlinear elastic elements, the characteristics of which are based on passive muscle behaviour. Thus, the muscle elements cannot adequately represent the tensed state of the muscles of the human volunteers subjected to sled acceleration tests. To express this tensed state, a force-displacement curve for active muscle behaviour may be applied. Ideally, a muscle model that can simulate muscle contraction should be employed, with which the effect of muscle contraction on the model response can be studied. Such a muscle model was used by Williams and Belytschko [18] in their finite element neck model, and they found a significant difference in response for simulations with and without muscle contraction.

VALIDATION Ideally, validation should be carried out at two levels. At a global level, the responses of the head relative to the torso are looked at, but the behaviour of the neck is not considered in detail. At a more detailed level, the vertebral kinematics are taken into account as well. Then the neck is not seen as a 'black box' guiding the head motion into the correct path, but intervertebral deformations are looked at as well. In the neck, especially in a mathematical model of it, a certain position and orientation of the head may be obtained by several different combinations of vertebral positions and orientations. The neck is modelled as a kinematically redundant system: each vertebra has 6 degrees of freedom (dofs), resulting in 42 dofs describing the 6 dofs of the head.

Thus, as part of a detailed validation, vertebral motions should be taken into account as well. Unfortunately, not many experiments have been reported that reveal vertebral motions in dynamic head-neck loading, let alone for impact situations similar to the sled tests. For example, Pintar *et al.* [8] have reported on vertebral motions for dynamic axial head impacts on head-neck specimens.

In the present study, the gross head-neck motion of the model was validated for frontal and lateral impacts and for both impacts qualitatively good correspondence with human volunteer response envelopes was found. However, for the frontal impact, the model showed almost no head lag as opposed to the volunteers. The lateral impacts are more difficult to predict than the frontal ones, due to the three-dimensional motion involved. Lateral bending of the neck is always associated with axial rotation of vertebrae and head due to the anatomical arrangement of the articular facet joints [35]. In principle, this coupling effect is included into the model by the non-diagonal stiffness coefficients in the joint model. However, it was found that the coupling coefficients currently used had only a moderate influence on the model response for both frontal and lateral impacts. This may be due to the fact that the coefficients were based on thoracic motion segments for which the coupling is less pronounced.

To obtain a general valid model, the model should

be validated for other impact directions and severities as well. Most importantly, the model response to low-speed rear-end impacts should be validated, as these impacts frequently occur and often result in neck injuries. Recently, Ono and Kanno [1] and McConnell *et al.* [36] have reported on low-speed rear-end impacts with human volunteers in which head and torso motion were monitored. Their results may be used for validation.

FUTURE ENHANCEMENTS Improvements as those discussed above will be carried out for the global model to complete the first phase. Then, the model will be refined by including more details. A more detailed representation of intervertebral joint behaviour is needed, to obtain a model that reveals soft tissue loads and, ultimately, injury mechanisms. This may be achieved by replacing the current intervertebral joint model by separate representations of the soft tissue components, i.e. different models for the intervertebral disc, ligaments, and facet joints. This will increase the model complexity greatly, as much more parameters are needed to describe, for example, the material behaviour and geometry of ligaments, discs, and articular facets. Consequently, model validation becomes more complex too. This will be part of the second phase of the two-phase approach.

SUMMARY AND CONCLUSIONS

- The discrete parameter head-neck model of Deng and Goldsmith was modified and implemented in MADYMO. The model comprises rigid head and vertebrae, connected by linear viscoelastic intervertebral joints, and several nonlinear elastic muscle elements.
- Modifications included:
  - a different representation of the muscles,
  - a modified joint model with respect to the used stiffness matrix,
  - modified values for the moments of inertia of vertebrae C4, C5, and C6, and
  - modified values for the mass and moments of inertia of the head (for the validation simulations only).
- The model response to a frontal and lateral impact was compared to the results given by Deng. The modified model showed similar response patterns as Deng's model, but was found to be more flexible, partly due to the differing muscle representation.
- To validate the model, responses were compared to human volunteer response envelopes for frontal and lateral impacts. For the frontal impact, fair agreement was found, except for the head lag that was not properly reflected by the model. This was thought to be due to inappropriate modelling of the atlanto-occipital joint. For the lateral impact, agreement between model and volunteer responses was good for the linear accelerations and displacements of the head cg, reasonable for the head angular accelerations, and insufficient for the head rotations.
- A sensitivity analysis was performed to assess the response sensitivity to parameter variations. It was found that variations in head mass as well as in joint stiffness and damping coefficients with respect to rotational deformations have a major influence on model response. The influence of variations of the joint proportionality factor and muscle stiffness was moderate, while the influence of vertebral mass variations was negligible. Omitting the coupling coefficients of the joint stiffness matrix influenced the model response moderately.
- Although amenable to enhancements, the model proved satisfactory in predicting human head-neck responses to frontal and lateral impacts. It may be used, for example, as a tool to improve restraint systems and dummy necks.

REFERENCES

[1] K. Ono and M. Kanno. Influences of the physical parameters on the risk to neck injuries in low impact speed rear-end collisions. In *International IRCOBI Conference on the Biomechanics of Impacts*, pages 201–212. IRCOBI, 1993.

[2] D. Otte and J.R. Rether. Risk and mechanisms of injuries to the cervical spine in traffic accidents. In *International IRCOBI Conference on the Biomechanics of Impacts*, pages 17–32. IRCOBI, 1985.

[3] G. Faverjon, C. Henry, C. Thomas, C. Tarrière, A. Patel, C. Got, and F. Guillon. Head and neck injuries for belted front occupants involved in real frontal crashes: Patterns and risks. In *International IRCOBI Conference on the Biomechanics of Impacts*, pages 301–317. IRCOBI, 1988.

[4] O. Bunketorp, B. Romanus, and P.O. Kroon. Head and neck injuries in traffic accidents in Göteborg in 1983. In *International IRCOBI Conference on the Biomechanics of Impacts*, pages 1–16. IRCOBI, 1985.

[5] P. Lövsund, A. Nygren, B. Salen, and C. Tingvall. Neck injuries in rear end collisions among front and rear seat occupants. In *International IRCOBI Conference on the Biomechanics of Impacts*, pages 219–326. IRCOBI, 1988.

[6] C. Deutscher. *Bewegungsablauf von Fahrzeuginsassen beim Heckaufprall. Ermittlung von objektiven Meßwerten zur Beurteilung von Verletzungsart und -schwere.* PhD thesis, Technische Universität München, 1993.

[7] R.W. Nightingale, B.J. Doherty, B.S. Myers, J.H. McElhaney, and W.J. Richardson. The influence of end condition on human cervical spine injury mechanisms. In *Proceedings of the 35th Stapp Car Crash Conference*, pages 391–399. Society of Automotive Engineers, 1991. SAE Paper No. 912915.

[8] F.A. Pintar, A. Sances Jr., N. Yoganandan, J. Reinartz, D.J. Maiman, J.K. Suh, G. Unger, J.F. Cusick, and S.J. Larson. Biodynamics of the total human cadaveric cervical spine. In *Proceedings of the 34th Stapp Car Crash Conference*, pages 55–72. Society of Automotive Engineers, 1990. SAE Paper No. 902309.

[9] T.R. Oxland and M.M. Panjabi. The onset and progression of spinal injury: A demonstration of neutral zone sensitivity. *Journal of Biomechanics*, 25:1165–1172, 1992.

[10] N. Yoganandan, J.B. Myklebust, G. Ray, and A. Sances Jr. Mathematical and finite element analysis of spine injuries. *CRC Critical Reviews in Biomedical Engineering*, 15:29–93, 1987.

[11] M. de Jager. Mathematical modelling of the human cervical spine: A survey of the literature. In *International IRCOBI Conference on the Biomechanics of Impacts*, pages 213–227. IRCOBI, 1993.

[12] C.C. Ward and G.K. Nagendra. Mathematical models: Animal and human models. In A.M. Nahum and J. Melvin, editors, *The Biomechanics of Trauma*, pages 77–100. Appleton-Century-Crofts, Norwalk, Connecticut, 1985.

[13] A.C. Bosio and B.M. Bowman. Simulation of head-neck dynamic response in -Gx and +Gy. In *Proceedings of the 30th Stapp Car Crash Conference*, pages 345–378. Society of Automotive Engineers, 1986. SAE Paper No. 861895.

[14] J. Wismans, E. van Oorschot, and H.J. Woltring. Omnidirectional human head-neck response. In *Proceedings of the 30th Stapp Car Crash Conference*. Society of Automotive Engineers, 1986. SAE Paper No. 861893.

[15] J. Wismans, M. Philippens, E. van Oorschot, D. Kallieris, and R. Mattern. Comparison of human volunteer and cadaver head-neck response in frontal flexion. In *Proceedings of the 31st Stapp Car Crash Conference*. Society of Automotive Engineers, 1987. SAE Paper No. 872194.

[16] C.S. Tien and R.L. Huston. Biodynamic modeling of the head/neck system. In *Field Accidents Data Collection Analysis, Methodologies and Crash Injury Reconstruction*, pages 359–364. Society of Automotive Engineers, 1985. SAE Special Publication P-159. Paper No. 850438.

[17] Y.C. Deng and W. Goldsmith. Response of a human head/neck/upper-torso replica to dynamic loading - II. analytical/numerical model. *Journal of Biomechanics*, 20:487–497, 1987.

[18] J.L. Williams and T.B. Belytschko. A three-dimensional model of the human cervical spine for impact simulation. *Journal of Biomechanical Engineering*, 105:321–331, 1983.

[19] M. Kleinberger. Application of finite element techniques to the study of cervical spine mechanics. In *Proceedings of the 37th Stapp Car Crash Conference*, pages 261–272. Society of Automotive Engineers, 1993. SAE Paper No. 933131.

[20] TNO Crash-Safety Research Centre, Delft, The Netherlands. *MADYMO User's Manual, Version 5.1*, 1994.

[21] Y.C. Deng. *Human Head/Neck/Upper-Torso Model Response to Dynamic Loading*. PhD thesis, University of California, Berkeley, 1985.

[22] Y.K. Liu, J.M. Laborde, and W. van Buskirk. Inertial properties of a segmented cadaver trunk: their implications in acceleration injuries. *Aerospace Medicine*, 42:650–657, 1971.

[23] J. Wittenburg. *Dynamics of Systems of Rigid Bodies*. Teubner, Stuttgart, 1977.

[24] M.M. Panjabi, R.A. Brand, and A.A. White III. Three-dimensional flexibility and stiffness properties of the human thoracic spine. *Journal of Biomechanics*, 9:185–192, 1976.

[25] H. Yamada. *Strength of Biological Materials*. Williams and Wilkins, Baltimore, 1970. Editor: F.G. Evans.

[26] C.L. Ewing and D.J. Thomas. Human head and neck response to impact acceleration. Monograph 21 USAARL 73-1, Naval Aerospace and Regional Medical Centre, Pensacola, 1972.

[27] J. Wismans and M. Beusenberg. Dummy-neck response requirements in frontal bending. Technical Report EEVC-WG12-DOC 15, TNO Crash-Safety Research Centre, Delft, The Netherlands, 1992.

[28] V.K. Goel, C.R. Clark, K. Gallaes, and Y.K. Liu. Moment-rotation relationships of the ligamentous occipito-atlanto-axial complex. *Journal of Biomechanics*, 21:673–680, 1988.

[29] H. Chang, L.G. Gilbertson, V.K. Goel, J.M. Winterbottom, C.C. Clark, and A. Patwardhan. Dynamic response of the occipito-atlanto-axial (C0-C1-C2) complex in right axial rotation. *Journal of Orthopaedic Research*, 10:446–453, 1992.

[30] M. Panjabi, J. Dvorak, J. Duranceau, I. Yamamoto, M. Gerber, W. Rausching, and H.U. Bueff. Three-dimensional movements of the upper cervical spine. *Spine*, 13:726–730, 1988.

[31] M.M. Panjabi, D.J. Summers, R.R. Pelker, T. Videman, G.E. Friedlaender, and W.O. Southwick. Three-dimensional load-displacement curves due to forces on the cervical spine. *Journal of Orthopaedic Research*, 4:152–161, 1986.

[32] S.P. Moroney, A.B. Schultz, J.A.A. Miller, B. Gunnar, and G.B.J. Andersson. Load-displacement properties of lower cervical spine motion segments. *Journal of Biomechanics*, 21:769–779, 1988.

[33] M. Shea, W.T. Edwards, A.A. White, and W.C. Hayes. Variations of stiffness and strength along the human cervical spine. *Journal of Biomechanics*, 24:95–107; 689–690, 1991.

[34] J.B. Myklebust, F. Pintar, N. Yoganandan, J.F. Cusick, D. Maiman, T.J. Myers, and A. Sances Jr. Tensile strength of spinal ligaments. *Spine*, 13:526–531, 1988.

[35] A.A. White III and M.M. Panjabi. *Clinical Biomechanics of the Spine*. J.B. Lippincott Company, Philadelphia, Toronto, 2nd edition, 1990.

[36] W.E. McConnell, R.P. Howard, H.M. Guzman, J.B. Bomar, J.H. Raddin, J.V. Benedict, H.L. Smith, and C.P. Hatsell. Analysis of human test subject kinematic responses to low velocity rear end impacts. In *Vehicle and Occupant Kinematics: Simulation and Modelling*, pages 21–30. Society of Automotive Engineers, 1993. SAE Special Publication SP-975, Paper No. 930889.

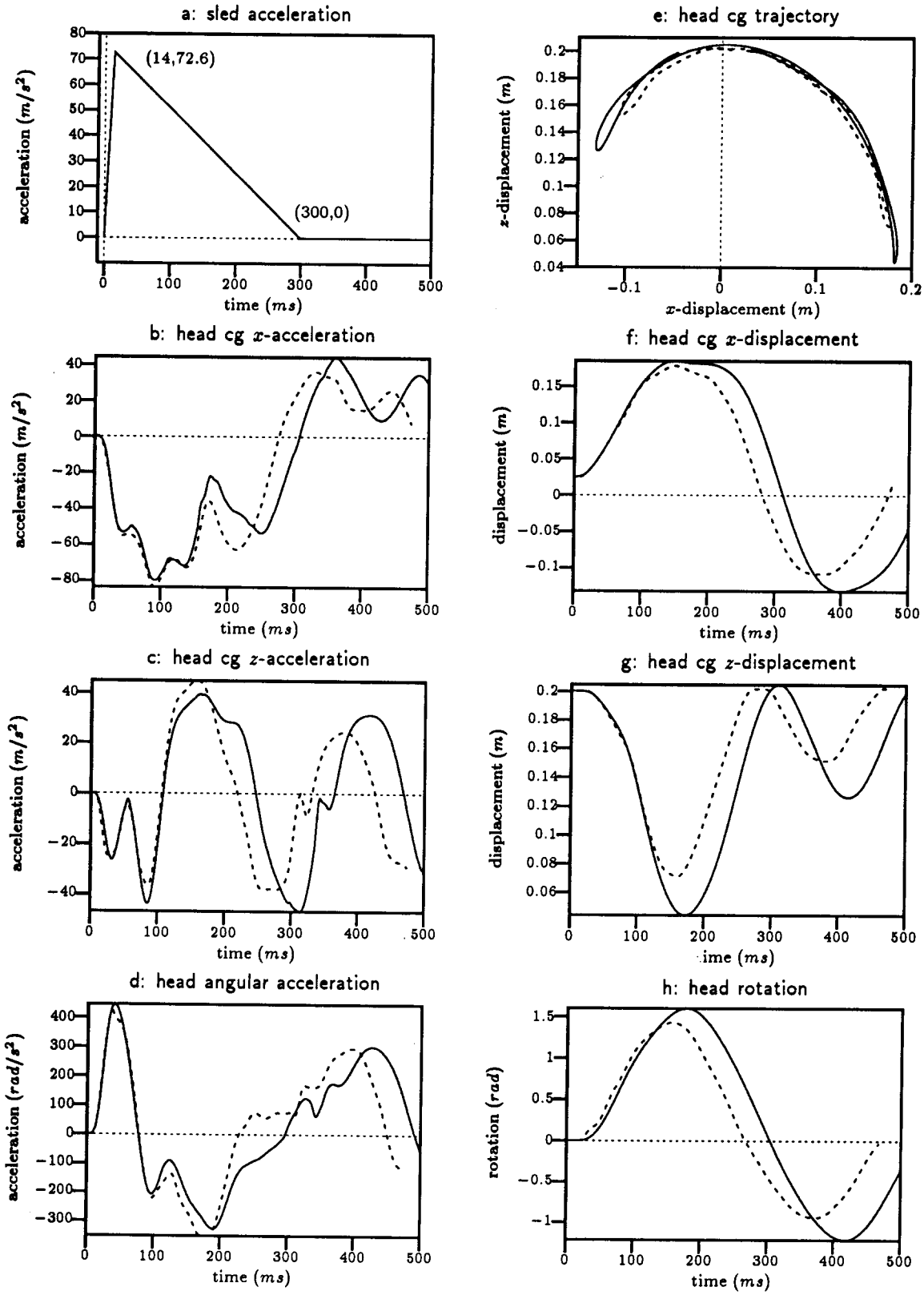

Figure 5: Response of Deng's model (- -) and present model (—) for Deng Frontal Impact.

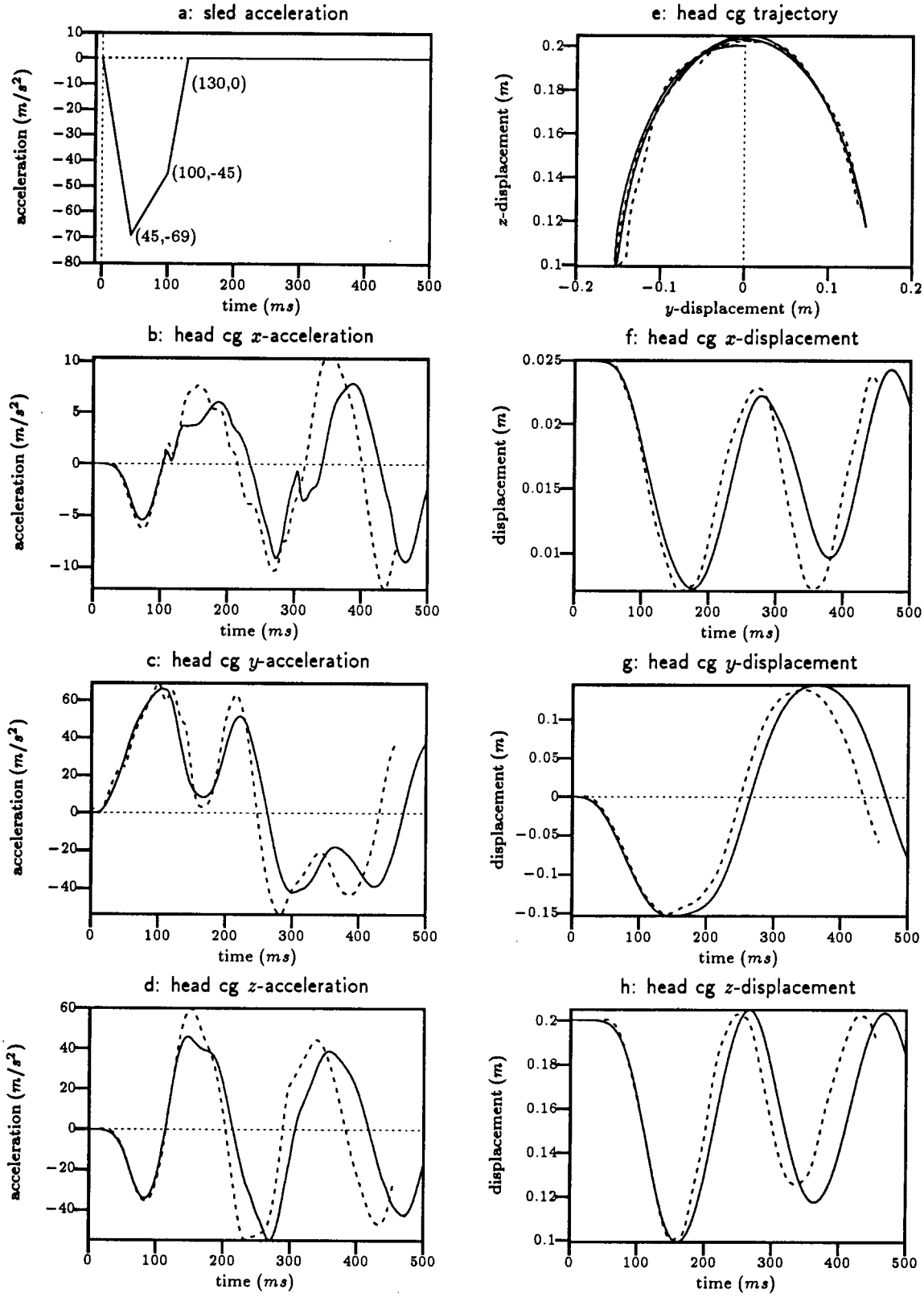

Figure 6: Response of Deng's model (- -) and present model (—) for Deng Lateral Impact.

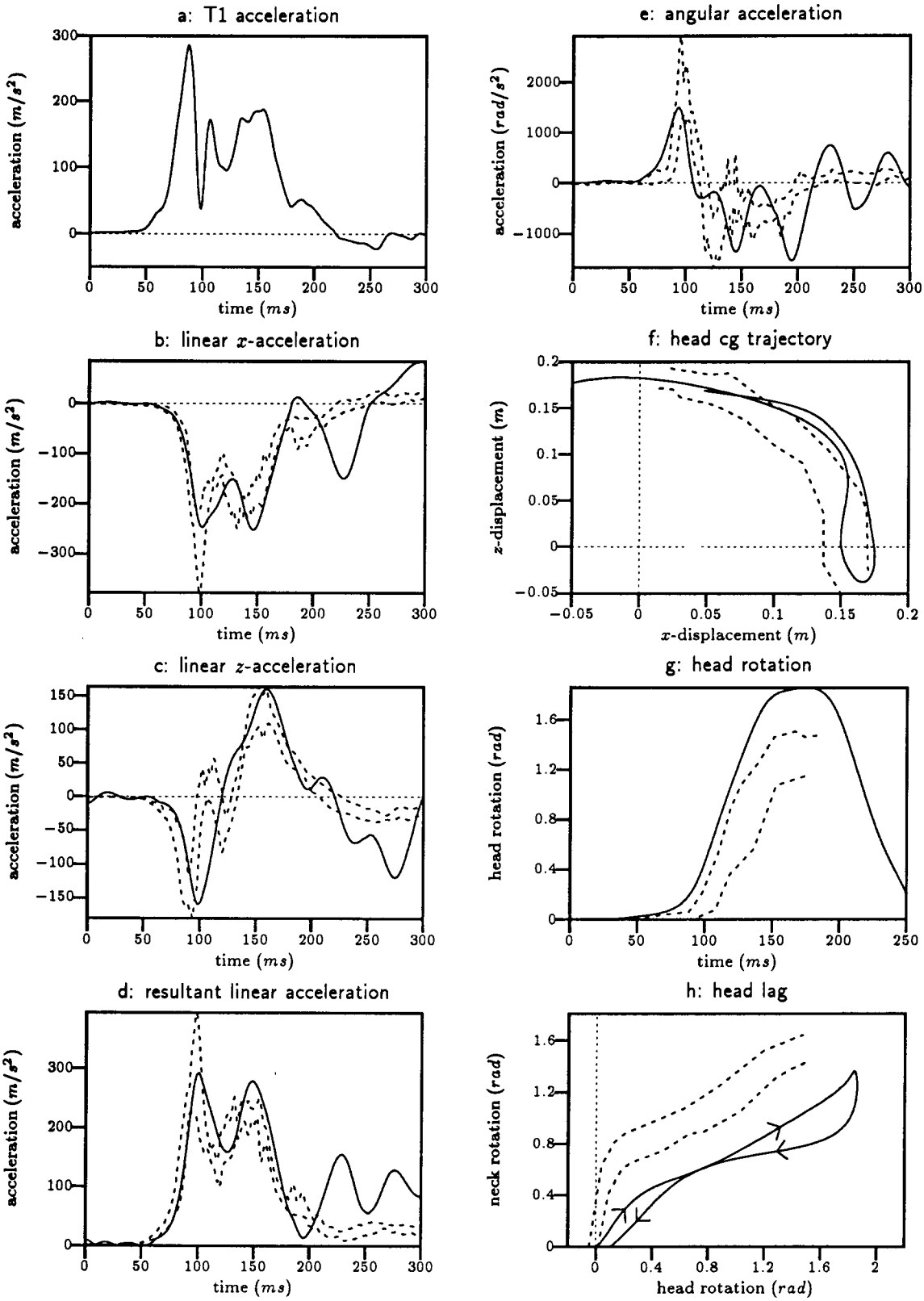

Figure 7: Model response (—) and volunteer envelopes (- -) for Volunteer Frontal Impact.

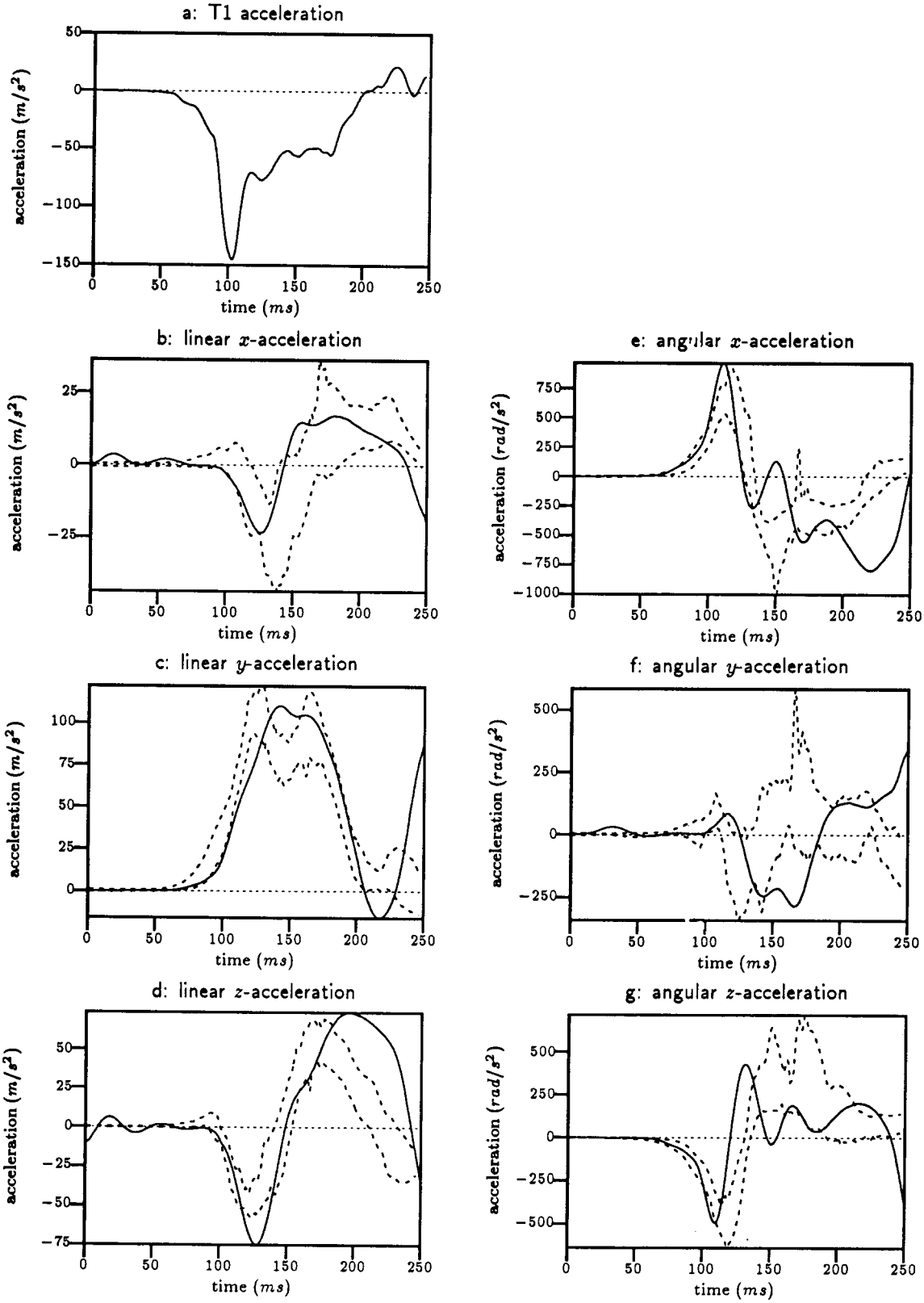

Figure 8: Model response (—) and volunteer envelopes (- -) for Volunteer Lateral Impact.

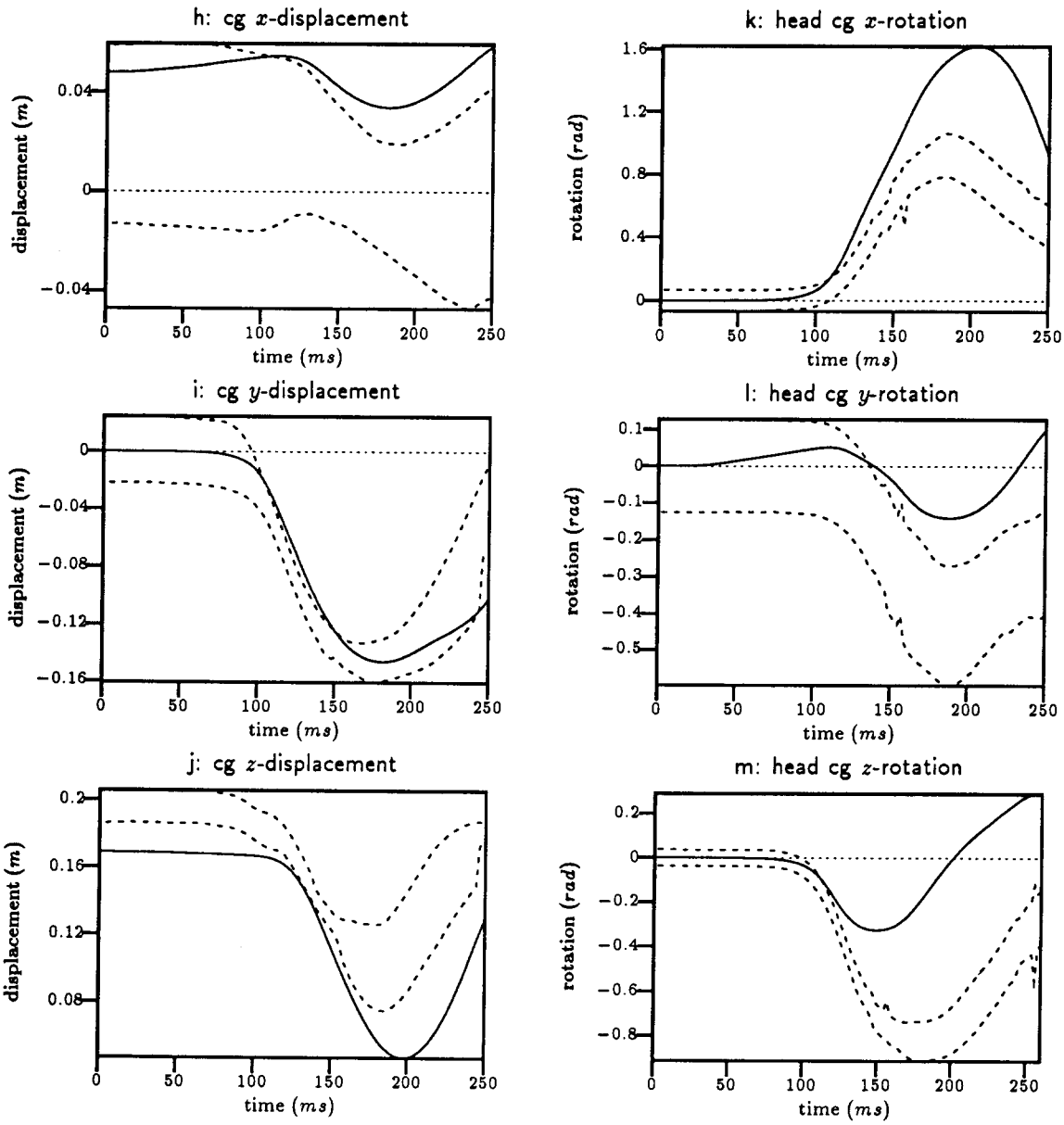

Figure 8: Model response (—) and volunteer envelopes (- -) for Volunteer Lateral Impact (continued).